Theor Chem Acc (2010) 125:419–426
DOI 10.1007/s00214-009-0680-3

REGULAR ARTICLE

Quantum chemical excited state calculations on pigment–protein complexes require thorough geometry re-optimization of experimental crystal structures

Andreas Dreuw · Philipp H. P. Harbach · Jan M. Mewes · Michael Wormit

Received: 27 April 2009 / Accepted: 31 October 2009 / Published online: 19 November 2009

Abstract Calculations of vertical excited states of a strongly coupled chlorophyll pair and a carotenoid–chlorophyll complex stemming from the light harvesting complex II of green plants employing the experimentally determined crystal structures and quantum chemically re-optimized model complexes demonstrate the need for preceding re-optimizations of the experimental structures at quantum chemical level. While in the case of the chlorophyll dimers, the re-optimization step is crucial for a correct description of the coupling of the excited states, in carotenoid–chlorophyll complexes the S_1 excitation energies of carotenoids depend strongly on the structure, in particular on the correct bond lengths alternation pattern of its conjugated double bond chain, which is not sufficiently accurately reproduced by experimental structures.

Keywords Light harvesting complexes · Geometry optimization · Quantum chemical calculations · Excited states · Excitation energy transfer · Electron transfer · Crystal structures

1 Introduction

Today, many experimental techniques are available to determine structures of biomolecules, e.g. proteins, protein complexes, DNA and many more. A short glance at the protein data base reveals the wealth of available experimentally determined structures. The most prominent experimental techniques for structure determination are X-ray crystallography and multi-dimensional NMR spectroscopy. These structures very often pave the road for a deeper understanding of the function of the corresponding biomolecule, in particular, when the function of the biomolecule is determined by the overall qualitative structure. This is typically not the case for enzymes and pigment proteins, whose functions are to catalyze a chemical reaction or to perform some light-driven processes, which both are quantum mechanical events. In such cases, small errors in bond lengths and angles can have an enormous effect on the energy of the involved molecules and as a consequence on the molecular mechanisms. Therefore, the accuracy of crystal structures of enzymes and pigment proteins are often not sufficient for a detailed molecular understanding of their function. As a consequence, crystal structures cannot directly be employed in quantum chemical calculations, but it is mandatory to re-optimize experimental structures when quantum mechanical questions are to be addressed. This is a well-known fact for enzyme catalysis, and here one usually resorts to QM/MM schemes, which couple a quantum mechanical treatment of the reactive region with a classical mechanics treatment of the surrounding protein, and solvent or membrane [1–3]. Although one can take for granted that experimental structures need to be re-optimized also for meaningful excited state calculations, it has not yet been demonstrated and clearly spelled out in the literature. This work may serve as a warning of what problems may occur, if a thorough quantum chemical re-optimization of experimentally determined structures of pigment proteins are omitted prior to excited state calculations (also if the environment is not properly taken into account).

Dedicated to Professor Sandor Suhai on the occasion of his 65th birthday and published as part of the Suhai Festschrift Issue.

A. Dreuw (✉) · P. H. P. Harbach · J. M. Mewes · M. Wormit
Institute of Physical and Theoretical Chemistry,
Goethe University Frankfurt, Max von Laue Str.7,
60438 Frankfurt, Germany
e-mail: andreas.dreuw@theochem.uni-frankfurt.de

One important class of pigment proteins are light harvesting complexes (LHC), which contain a large number of pigments typically chlorophylls and carotenoids. LHCs have been identified in all organisms performing photosynthesis, i.e. plants, purple bacteria and algae [4] being responsible for efficient absorption of light, the transport of excitation energy to the corresponding reaction centers [5, 6] and for quenching excess energy under high-light conditions [7–11]. Their function is determined by energy and electron transfer processes. It is obvious that the efficiencies of these processes are dictated by the interactions of the pigments, which are individually finely tuned by their relative structural arrangement in the LHCs, see for example the complex structure of LHC-II of green plants (Fig. 1) [12, 13]. In general, subtle geometric changes of the pigment structure and of their relative orientations can have a large influence on the excitation energies and the interaction of two pigments and thus on energy and electron transfer. It is thus crucially important to have a correct geometrical structure for a meaningful quantum chemical investigation of these processes, which generally requires excited state calculations. In particular, the correct bond length pattern of the conjugated π-systems of the involved pigments must be given with high accuracy since they strongly influence excitation energies.

Experimentally determined structures of large proteins typically exhibit resolutions of 1.5–3 Å, which is sufficiently accurate to determine the relative orientation of the pigments. Crystal structures are determined from an experimental set of phases, which serve as input for the calculation of a three-dimensional electron density map of the protein structure. However, even if an experimental resolution of 1.5 Å is reached, it is usually not unambiguously defined where to place the atoms. Methods to improve the density map rely on known structure data of the contained molecules, and typically, molecular modeling programs are used to refine the structure models using force fields within a minimization process. However, the obtained structures are usually affected with errors that are too large for the given pigment geometries to be directly employed for a meaningful quantum chemical calculation of excited states. Thus, the pigment structure needs to be re-optimized at reasonable levels of quantum chemistry. However, if energy or electron transfer between pigments of a LHC, for example, are in the focus of the investigation, the relative orientation of the pigments must be retained in the course of the geometry optimization, since the latter determines the pigment–pigment interactions.

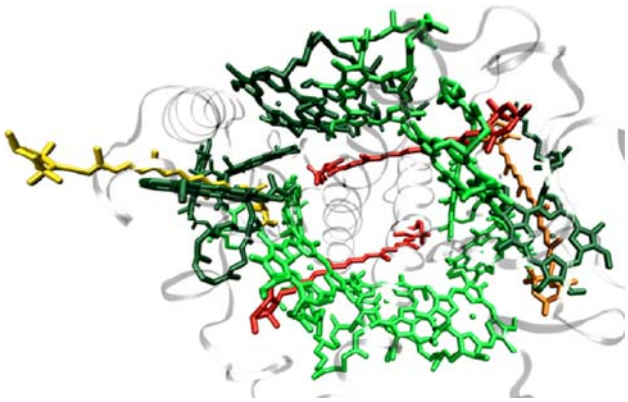

Fig. 1 Structural arrangement of the pigments in one monomer of the trimeric light harvesting complexes LHCII of green plants (*yellow* neoxanthin, *orange* violaxanthin, *red* lutein, *dark green* Chl *b*, *light green* Chl *a*)

In this contribution, the importance of the geometry optimization for meaningful calculations of excited state properties of the pigments and the errors that can occur when the re-optimization step is omitted are highlighted using two examples: a strongly coupled chlorophyll pair (Chl2 and Chl7 from LHC-II) and a lutein–chlorophyll complex (Lut1 and Chl2 also from LHC-II).

2 Theoretical methodology

Since the complete LHCs are too large to be treated quantum mechanically as a whole, the first step of investigations of their excitation energy and electron transfer properties is the construction of reduced molecular models that contain the relevant pigment–pigment interactions. Here, the known crystal structure of the LHC-II of green plants serves as input [10]. The set-up and the resulting structures of the molecular models are described in detail in later sections. Of course, it would be highly desirable to perform QM/MM calculations for the geometry optimization step, however, no reasonable force-field parametrization for light harvesting pigments, in particular for carotenoids, is currently available. In fact, we are at present working ourselves on development of a force filed for carotenoids. Therefore, the protein environment and hence its direct influence is for now generally neglected within our calculations unless mentioned otherwise. To include, however, the steric restrictions of the protein onto the pigments, selected geometric constraints are introduced within the geometry optimization to retain the relative orientations of the pigments in the designed model complexes. For their optimization, Kohn–Sham density functional theory has been used in combination with the well-known BLYP [14], and B3LYP [15] exchange–correlation (xc) functional and the 3-21G or SVP basis set as implemented in the Q-Chem 3.0 and Orca packages of ab initio programs [16, 17]. In the case of the Chl2·Chl7 chlorophyll dimer, the geometry has also been optimized using the BLYP xc-functional in combination with the additive dispersion correction devised by Grimme [18].

The developed model complexes have been used to calculate the lowest relevant electronic excited states using time-dependent density functional theory (TDDFT) [19, 20] and its Tamm-Dancoff approximation [21] in combination with the BLYP [14] xc-functional. This methodology has been shown previously to yield reasonable results for the excitation energies for the S_1 state of carotenoids as well as for the Q_y state of Chls [22–24] owing to fortuitous cancelation of errors [25]. However, excited charge transfer (CT) states suffer from electron transfer self-interaction in TDDFT and are given at much too low excitation energies and with a wrong asymptotic behavior with respect to a distance coordinate between electron donating and accepting groups [20, 26, 27]. Therefore, in the discussion of the locally excited $\pi\pi^*$ states, i.e. the S_1, S_2 states of carotenoids and the Q-states of the chlorophylls, the spurious CT states are generally discarded.

3 Results and discussion

3.1 Influence of individual geometrical parameters on the excitonic coupling and static absorption spectra of coupled chlorophyll dimers

One monomer of the otherwise trimeric LHC-II of green plants contains 14 chlorophyll and 4 carotenoid molecules, which are all involved in the light harvesting function of the pigment protein (Fig. 1). Due to the close packing of the pigments, it is clear that they are coupled to each other thus functioning as essentially one antenna. One of the most strongly coupled pigment pairs in the complex is the Chl2·Chl7 pair of chlorophyll *a* (Chl *a*) molecules. It is well-known from molecular biological deletion experiments that the Chl2 molecule (or the coupled pair) is the final acceptor of the harvested excitation energy and that from there the energy is funnelled further towards the photosynthetic reaction center. This strongly coupled Chl2·Chl7 chlorophyll pair serves in the following as an example to demonstrate that the accuracy of available crystal structure data is not sufficient to directly calculate absorption spectra and coupling strengths from the coordinates taken from the corresponding pdb-file (PDB-ID: 2bhw; see [13]).

As a first step in our theoretical calculation, the structure of the Chl2·Chl7 pair is taken from the crystal structure and the non-resolved, missing hydrogen atoms are added. While all other geometrical parameters are kept frozen, the ones of the newly added hydrogen atoms are optimized using standard KS-DFT/BLYP/SVP theory. Following this procedure, a Chl2·Chl7 model complex is obtained that most precisely reflects the structure of the X-ray data. As second step, this Chl2·Chl7 model complex serves as input for a constrained geometry optimization, in which all individual geometrical parameters of Chl2 and Chl7 are optimized using the BLYP xc-functional on one hand and the BLYP functional plus the long-range correction for dispersion (BLYP-D) on the other. During this step, however, it is important to preserve the relative orientation of the chlorophylls since this is crucial for their excitonic coupling and thus their absorption spectra. It turned out that the definition of a few intermolecular coordinates between the central four nitrogen atoms of the two chlorophylls offers a convenient and general way to maintain the relative orientation between them. Therefore, the distances N3-N6 (10.45 Å) as well as N2-N7 (8.81 Å), N1-N5 (9.95 Å) and N4-N8 (9.52 Å) are kept constant at the value of the crystal structure. For the definition of the numbering scheme see Scheme 1. Also the angles between N6-N7-N2 (94.02°), N3-N2-N7 (107.28°) and N8-N5-N1 (139.88°), N4-N1-N5 (16.59°) are frozen as well as the dihedral angles N3-N2-N7-N6 (17.65°) and N8-N5-N1-N4 (68.53°). The choice of the constraint is not unique, however, the chosen ones seem to be particularly practical. The results, however, are not sensitive with respect to the chosen constraints as long as the relative orientation of the pigments is conserved. Following this procedure, two further model complexes are obtained, one obtained at BLYP the other at BLYP-D level of theory. However, all three model complexes are practically indistinguishable with the naked eye (Fig. 2). Taking a closer look at the structures, the dispersion correction leads to a bending of the Chl planes similar to the crystal structure. This can be seen in Fig. 2 where the planes of the molecules overlap and intermolecular forces come to play. While the yellow and blue (BLYP-D, PDB) Chls are bending towards each other, the red (BLYP) structure shows the largest distance forming a perfect plane. This can be explained by the neglect of the medium-ranged van der Waals interactions in the original BLYP functional. The additive dispersion correction

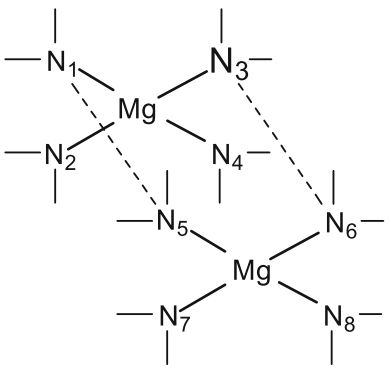

Scheme 1 Definition of the numbering scheme of the central nitrogen atoms

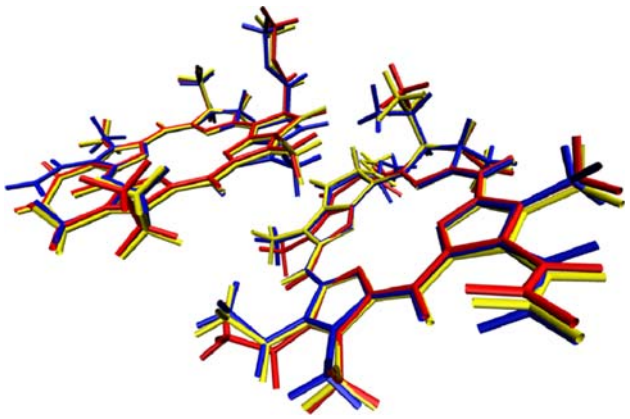

Fig. 2 Overlay of the structures of the three different Chl2·Chl7 model complexes: original crystal structure data (*blue*), re-optimized with constraints retaining the relative orientation using DFT/BLYP (*red*) and DFT/BLYP-D (*yellow*)

Table 1 Eight energetically lowest vertical excited states of the strongly coupled Chl2·Chl7 pair of LHC-II at the geometry of the crystal structure directly taken from the corresponding pdb-file and in the relative orientation of the crystal structure with geometries of the individual chlorophylls re-optimized at DFT/BLYP and DFT/BLYP-D level of theory

State	ω_{ex} [eV] (Osc.)		ω_{ex} [eV] (Osc.)		ω_{ex} [eV] (Osc.)	
	PDB		BLYP		BLYP-D	
S_1	1.41 (0.01)	CT	1.36 (0.00)	CT	1.44 (0.00)	CT
S_2	1.57 (0.00)	CT	1.53 (0.00)	CT	1.56 (0.00)	CT
S_3	1.66 (0.02)	CT	1.66 (0.00)	CT	1.62 (0.00)	CT
S_4	1.89 (0.00)	CT	1.82 (0.00)	CT	1.72 (0.00)	CT
S_5	2.03 (0.26)	$Q_{y(A)}$	2.01 (0.00)	CT	2.05 (0.41)	$Q_{y(+)}$
S_6	2.05 (0.23)	$Q_{y(B)}$	2.07 (0.34)	$Q_{y(+)}$	2.07 (0.03)	CT
S_7	2.06 (0.02)	CT	2.10 (0.00)	CT	2.09 (0.02)	CT
S_8	2.11 (0.01)	CT	2.10 (0.06)	$Q_{y(-)}$	2.10 (0.03)	$Q_{y(-)}$

re-introduces these attracting effects in an empirical way, leading to the described changes in the geometry.

As much as the overall geometries of the model complexes differ, the computed vertical excitation energies as obtained vary at TDDFT/BLYP/SVP level of theory (Table 1). For all model complexes, a plethora of spurious charge-transfer states is found, which are all given at much too low energy due to the well-known charge-transfer (CT) failure of TDDFT [26, 27]. Nevertheless, the excitation energies of these false states have also different values for the three model complexes pointing already out the influence of the individual geometrical parameters of the chlorophyll molecules Chl2 and Chl7. For example, the lowest excited S_1 state of all model complexes corresponds to a long-range CT state, in which an electron is excited from the highest occupied molecular orbital (HOMO) to the lowest unoccupied molecular orbital (LUMO), which

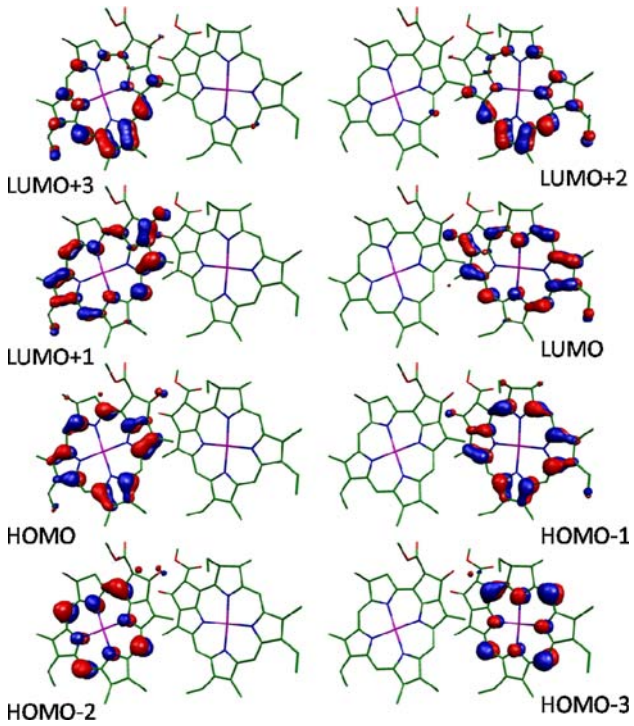

Fig. 3 Relevant molecular orbitals for the assignment of the Q_y states as obtained at the level of DFT/BLYP. In all model complexes, the orbitals are localized on either one of the chlorophylls and not delocalized over both. The *left* and *right panel* corresponds to the so-called Gouterman orbitals of Chl2 and Chl7, respectively

are localized on Chl2 and Chl7, respectively, i.e. an electron is transferred from Chl2 to Chl7 (Fig. 3). The excitation energy of this state is given at 1.41, 1.36 and 1.44 eV for the PDB-model, the BLYP-model and the BLYP-D-model, respectively (Table 1). However, all the CT states have no oscillator strength and they do also not mix with the locally excited $\pi\pi^*$ (Q_y) states. They do not contribute to the absorption spectrum and to excitation energy transfer properties of the Chl2·Chl7 dimer since those are dominated by the Q_y states. In the PDB-model, the latter are found as S_5 and S_6 at 2.03 and 2.05 eV, respectively (Table 1). Analysis of the wavefunctions and coupling between these states reveals that they are practically not coupled, since each chlorophyll molecule exhibits its own Q_y state with its original oscillator strength. The wavefunctions of the Q_y states correspond to linear combinations of Slater determinants that are only located on one of the Chl molecules, i.e. neither the molecular orbitals are de-localized nor are the typical positive and negative linear combinations of the individual excited states found, which would be present in the excitonically coupled case. This manifests itself also directly in the theoretical absorption spectrum of the PDB-model which is depicted in Fig. 4. Two peaks with almost identical oscillator strength are seen, and not one peak carrying the sum of the

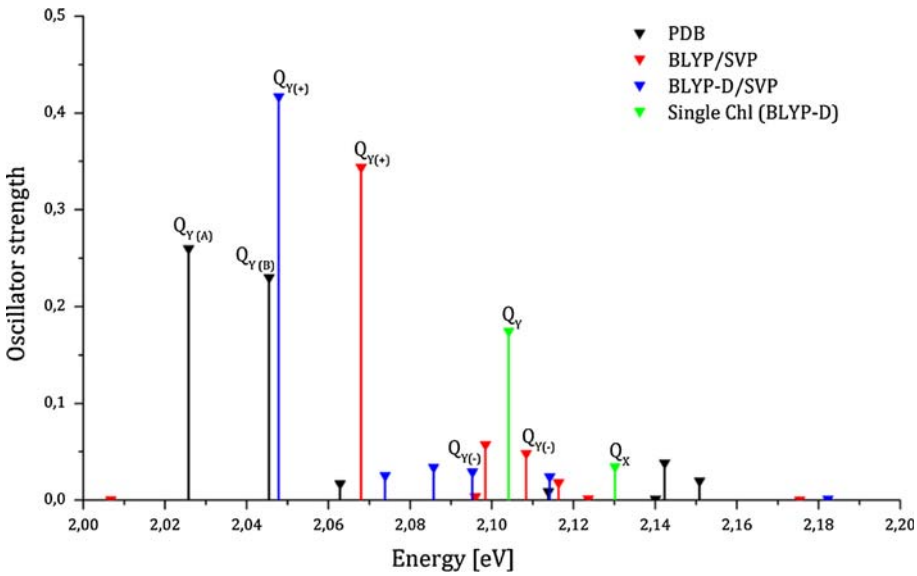

Fig. 4 Stick representation of the computed absorption spectra in the region of the Q_y states of the Chl2·Chl7 model complexes as obtained from the crystal structure (*black*), from the re-optimized complexes using DFT/BLYP (*red*) and DFT/BLYP-D (*blue*) as well as for the individual chlorophylls optimized with DFT/BLYP-D (*green*)

strengths of both states as it would be in a strongly coupled case. The situation changes drastically for the re-optimized BLYP- and BLYP-D-models. Here, the Q_y states are given as S_6 and S_8 at 2.07 and 2.10 eV in the BLYP-model and as S_5 and S_8 at 2.05 and 2.10 eV in the BLYP-D-model, respectively, that is with only minor differences. It is immediately apparent that the energetically lowest Q_y states of these models have large oscillator strength while the energetically higher one have practically none. This already hints at a strong coupling of these states and this is indeed further corroborated by analyses of the corresponding wavefunctions. In these cases, they are represented by positive and negative linear combinations of determinants that are located on different Chls, i.e. they are linear combinations of the local Q_y states, precisely how one would expect for an excitonically coupled system. Therefore, they are denoted as $Q_y(+)$ and $Q_y(-)$ in Table 1 and Fig. 4. Also in the calculated absorption spectra, the typical pattern of excitonically coupled states is found for the BLYP- and BLYP-D-model complexes: one peak with all oscillator strength and one with essentially none. For comparison, also the excitation spectra of the individual Chl2 and Chl7 have been computed individually and are plotted in Fig. 4.

It is worthwhile to note that the Q_y states are obtained with excitation energies of 2.11 and 2.15 eV when the structure of the chlorophyll dimer is optimized employing the B3LYP xc-functional, i.e. they are shifted to slightly larger values. Nevertheless, also in this case, the lower state is a positive linear combination of the individual states and exhibits the complete oscillator strength of both while the one with the higher excitation energy is the corresponding negative combination having no strength.

Summarizing our findings for the Chl2·Chl7 dimer of LHC-II, it has been demonstrated that a careful re-optimization of the crystal structure data is essential for the correct theoretical description of the excited states of the individual pigments and in particular of their coupling. For the correct description of the latter, however, great care must be taken that the relative orientation of the pigments remains conserved during the structure optimization since the orientation of the transition dipole moments is crucial for the coupling of the Q_y states. In the case of the Chl2·Chl7 dimer, re-optimization of the individual pigments has a significant influence on the coupling between them. While the PDB-model exhibiting the original crystal structure resembles a system of practically uncoupled Chls, the re-optimized models describe a strongly coupled pair of Chls. Since it is experimentally well-known that Chl2 and Chl7 of LHC-II are in fact strongly coupled, it becomes now undoubtedly clear that re-optimization of crystal structures is indispensible for the development of model complexes capturing the correct excited state properties of coupled dimers.

3.2 Excited states of the central lutein–chlorophyll pair of LHC-II

Other useful examples for the importance of quantum chemical structure re-optimization of experimental crystal structures prior to excited state calculations are carotenoid–chlorophyll complexes, which are ubiquitous in LHCs. Besides absorption of light, carotenoids fulfill important protective functions. They scavenge singlet oxygen and quench triplet chlorophyll states as well as excess excitation energy. For a detailed understanding of the molecular mechanisms of these functions, precise knowledge of the

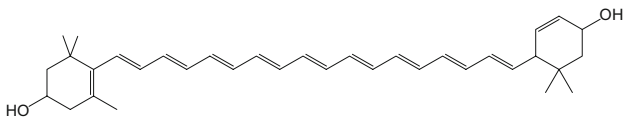

Scheme 2 Molecular structure of lutein

excited states of the carotenoids and chlorophylls within their complexes is of utmost importance.

In one monomer of LHC-II of green plants, three different kinds of carotenoids are present: two lutein molecules, one violaxanthin and one neoxanthin. However, here we focus on the excited states of a complex between lutein 1 (Lut1) (Scheme 2) and chlorophyll Chl2, which was already topic of the previous section. This complex is at the core of LHC-II (Fig. 1), and the interaction between these pigments is known to be important for triplet quenching. However, lately it has also been suggested that they might also be involved in excess singlet energy quenching [28, 29]. Therefore, the calculation of the singlet excited states of this complex as well as an investigation of the nature of the interaction of Lut1 and Chl2 is required to obtain insight into possible molecular quenching mechanisms. However, in this work we aim at demonstrating the importance of geometry re-optimization for the correct theoretical description of the excited states and not so much on the function of Lut1 in LHC-II.

As first step of our theoretical investigation, the *xyz*-coordinates of the Lut1·Chl2 complex have been taken from the pdb-file of the corresponding crystal structure [13]. Hydrogen atoms have been added and their positions were re-optimized at the theoretical level of DFT/B3LYP/6-31G*, while all heavy atoms were kept at their original positions. This procedure gives rise to our first model complex, the PDB-model (Fig. 5). Secondly, the PDB-model serves as input for a structure re-optimization of the pigments at DFT/B3LYP/6-31G* level of theory resulting in the second B3LYP-model. Similar to the optimization of the chlorophyll pair described in the previous section, also here it is important to preserve the relative orientation of Lut1 and Chl2 in the course of the re-optimization step. This is again guaranteed through the introduction of constraints on intermolecular geometrical parameters. In general, it is more involved to develop reasonable constraints for a carotenoid-chlorophyll complex than for a chlorophyll pair, and it is practically impossible to derive a generalized prescription. This difficulty is mostly related to the flexibility of the carotenoid molecule, which adopts a certain molecular configuration, i.e. bending and twisting of the conjugated polyene chain, within the protein induced by spatial restrictions. If one wishes to reproduce those, too, one needs then to introduce also intramolecular constraints on the carotenoid side. The philosophy that we

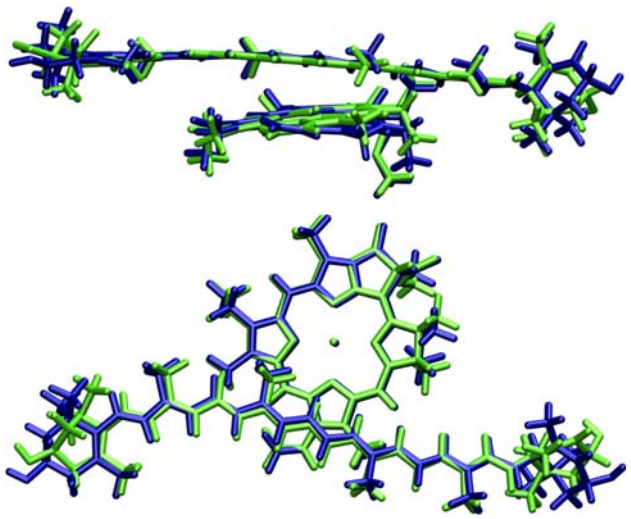

Fig. 5 Overlay of the crystal structure (PDB-model) of the Lut1·Chl2 complex (*blue*) with the re-optimized B3LYP-model complex (*green*)

follow in the derivation of those geometry constraints is to set up as many as necessary but as little as possible to conserve the most important features of the complex, i.e. relative orientation of the pigments and the bending and twisting of the carotenoid. For the Lut1·Chl2 complex (Fig. 5), this amounts to altogether six angles and ten dihedrals. Interestingly, the intermolecular distance between Lut1 and Chl2 needs not to be restricted. It changes only negligibly from 4.09 to 4.17 Å upon optimization. An overlay of the structures of the two model complexes is displayed in Fig. 5. For the Lut1·Chl2 complex, we have chosen to optimize the geometry at DFT/B3LYP/6-31G* level, since the B3LYP xc-functional has proven to yield very reasonable geometrical parameters in particular for the conjugated carbon–carbon bond lengths of the carotenoid [30], while BLYP tends to overestimate bond length equilibration [31]. Furthermore, the use of BLYP-D for the geometry optimization of the Lut1·Chl2 complex leads to a strong bending of Lut1 "embracing" the Chl2 molecule. This is not possible in the LHC due to steric hinderance by the protein. Therefore, we discard this structure from further discussions.

In the case of the Lut1·Chl2 complex, the re-optimization procedure has a larger influence on the excitation energies of the pigments than in the case of the Chl2·Chl7 chlorophyll pair described above, which have been computed employing TDDFT/BLYP/3-21G. We have chosen this xc-functional/basis set combination since it has been shown previously that it yields S_1 excitation energy of carotenoids in very good agreement with the best known experimental values [24]. Different xc-functional/basis set combinations usually fail to give even the correct ordering of the carotenoid excited S_1 and S_2 states [22]. Again, a plethora of intermolecular excited charge-transfer states is

Table 2 Excitation energies of the locally excited S_1 and S_2 states of Lut1 and of the Q_y and Q_x states of Chl2 as computed for the PDB-model complex and for the B3LYP model at the theoretical level of TDDFT/BLYP/3-21G

State	ω_{ex} [eV]	
	PDB	B3LYP
S_1(Car)	1.86	2.07
Q_y (Chl)	2.13	2.19
Q_x (Chl)	2.26	2.22
S_2 (Car)	2.29	2.28

found, which are far too low in energy and thus discarded from the discussion. This phenomenon has been observed and documented previously several times [24, 32–34]. Surprisingly, when the PDB-model is used for the calculation of the excited states also several intramolecular excited charge-transfer states are identified on Lut1. These states correspond to $n\pi^*$-excitations of an electron from an oxygen lone-pair orbital and to $\pi\pi^*$-excitations of the π-orbitals of the isolated β-ionone ring double bond into a π^*-orbital of the conjugated chain. However, these states are also artificially too low by approximately 1–1.5 eV and can also be discarded from the discussion. Let us thus focus on the excited states of the complex that are relevant for excitation energy transfer between Lut1 and Chl2, i.e. those which correspond to the S_1 and S_2 states of Lut1 and the Q_y and Q_x states of Chl2.

Inspecting the vertical excitation energies obtained at the theoretical level of TDDFT/BLYP/3-21G for the PDB-model and the B3LYP-model (Table 2), one recognizes immediately that the influence of the geometry optimization is only small for the Q_y and Q_x states of Chl2 and for the S_2 state of Lut1. Most notably, however, is the significant change in excitation energy of the S_1 state of Lut1. For the PDB-structure the vertical excitation energy is only 1.86 eV, while it is increased by 0.21–2.07 eV when the re-optimized B3LYP-model is employed in the calculation. This is a very important energetic contribution, since the S_1 state of Lut1 is the crucial state for the energy transfer processes to or from Chl2. The change in the excitation energy is mostly due to a better description of the bond length pattern of the conjugated chain of Lut1 with DFT/B3LYP than is given by the crystal structure. This highlights once more the sensitivity of the S_1 excited state of carotenoids with respect to the geometrical structure, in particular with respect to the conjugated bond length pattern [31]. For such sensitive cases, the accuracies of crystal structures of pigment proteins are simply not high enough to allow for a direct application in excited state calculations. Of course, also the structures optimized at DFT/B3LYP level of theory exhibit errors, however, they can be expected to be significantly smaller than the experimental ones stemming from fitting the experimentally determined electron density map to common characteristics of known molecular data and refinement with classical force field approaches.

4 Concluding remarks

Using the strongly coupled chlorophyll dimer of Chl2 and Chl7 and the lutein–chlorophyll complex of Lut1 and Chl2 of LHC-II as typical examples, it has been demonstrated that the accuracy of the experimental crystal structure of LHC-II is not sufficient for the pigments to be directly employed in quantum chemical excited state calculations. In the case of the Chl2·Chl7 complex, the excited state calculations on the crystal structure yields states that resemble a pair of uncoupled chlorophylls, while upon constrained geometry optimization the chlorophylls Chl2 and Chl7 become strongly coupled, in agreement with well-known experimental findings [35–37]. A similar conclusion can be drawn for the results of the excited state calculations on the Lut1·Chl2 complex. Here, the geometry re-optimization has a large influence on the excitation energy of the S_1 state of Lut1, which is very sensitive with respect to the detailed structure of the conjugated bond length pattern. Re-optimization of the geometry improves significantly the experimental crystal structure and leads to a 0.2 eV shift of the S_1 excitation energy upwards. These educative examples may serve as a warning what kind of errors can occur when quantum chemical re-optimization of crystal structures is omitted prior to excited state calculations.

Very often in quantum chemistry one relies on error compensation, in particular, when relative energies, i.e. energy differences are studied. Thus, one might have hoped that this would also be the case when experimental crystal structures are directly employed in quantum chemical calculations, such that the error in the geometries of all pigments is roughly the same and cancels when excited states of pigments and pigment pairs are computed. This, however, seems not generally to be the case, and instead the errors persist. In view of these findings, re-optimization of the structures employing quantum chemical methods are indispensible for a proper description of excited states and their properties of the involved pigments. In the future, this methodology needs to be extended to QM/MM calculations, where the structure of pigment pairs or clusters of pigments can be re-optimized in the presence of the protein environment and other surrounding pigments. Then tedious inclusion of optimization constraints can be avoided and the direct structural and electrostatic influence of the environment can be included. However, the changes in the excitation energies are probably only small since the interior of LHC-II is highly unpolar.

Acknowledgments A.D. gratefully acknowledges financial support by the German Science Foundation as Heisenberg-Professor.

References

1. Friesner RA, Guallar V (2005) Annu Rev Phys Chem 56:389–427
2. Lin H, Truhlar DG (2007) Theor Chem Acc 117:185–199
3. Senn HM, Thiel W (2007) Curr Opin Chem Biol 11:182–187
4. Green BR, Parson WW (2003) Light-harvesting antennas in photosynthesis. Kluwer Academic Publisher, Dordrecht
5. van Amerongen H, Dekker JP (2003) Light harvesting in photosystem II. In: Green BR, Parson WW (eds) Light-harvesting antennas in photosynthesis. Kluwer Academic Publishers, Dordrecht, pp 219–251
6. Allen JF, Forsberg J (2001) Trends Plant Sci 6:317–326
7. Demmig B, Winter K, Krüger A, Czygan F-C (1987) Plant Physiol 84:218–224
8. Horton P, Ruban AV, Walters RG (1996) Annu Rev Plant Physiol Plant Mol Biol 47:665–684
9. Niyogi KK (1999) Annu Rev Plant Physiol Plant Mol Biol 50:333–359
10. Kühlheim C, Ågren S, Jansson S (2002) Science 297:91–93
11. Holt NE, Fleming GR, Niyogi KK (2004) Biochemistry 43:8281–8289
12. Liu Z, Yan H, Wang K, Kuang T, Zhang J, Gui L, An X, Chang W (2004) Nature 428:287–292
13. Standfuss J, van Scheltinga ATerwisscha, Lamborghini M, Kühlbrandt W (2005) EMBO J 24:919–928
14. Becke AD (1988) Phys Rev A 38:3098
15. Becke AD (1993) J Chem Phys 98:5648
16. Shao Y, Molnar LF, Jung Y, Kussmann J, Ochsenfeld C, Brown ST, Gilbert ATB, Slipchenko LV, Levchenko SV, O'Neill DP, DiStasio RA, Lochan RC, Wang T, Beran GJO, Besley NA, Herbert JM, Lin CY, Van Voorhis T, Chien SH, Sodt A, Steele RP, Rassolov VA, Maslen PE, Korambath PP, Adamson RD, Austin B, Baker J, Byrd EFC, Dachsel H, Doerksen RJ, Dreuw A, Dunietz BD, Dutoi AD, Furlani TR, Gwaltney SR, Heyden A, Hirata S, Hsu CP, Kedziora G, Khalliulin RZ, Klunzinger P, Lee AM, Lee MS, Liang W, Lotan I, Nair N, Peters B, Proynov EI, Pieniazek PA, Rhee YM, Ritchie J, Rosta E, Sherrill CD, Simmonett AC, Subotnik JE, Woodcock HL, Zhang W, Bell AT, Chakraborty AK, Chipman DM, Keil FJ, Warshel A, Hehre WJ, Schaefer HF, Kong J, Krylov AI, Gill PMW, Head-Gordon M (2006) Phys Chem Chem Phys 8:3172
17. Neese F (2006) Orca Quantum Chemistry Package, Version 2.6.35. University of Bonn, Germany
18. Grimme S (2006) J Comput Chem 27:1787
19. Casida ME (1995) In: Chong DP (ed) Recent advances in density functional methods part I. World Scientific, Singapore, pp 155–192
20. Dreuw A, Head-Gordon M (2005) Chem Rev 105:4007
21. Hirata S, Head-Gordon M (1999) Chem Phys Lett 314:291
22. Hsu CP, Hirata S, Head-Gordon M (2001) J Phys Chem A 105:451
23. Dreuw A, Fleming GR, Head-Gordon M (2003) J Phys Chem B 107:6500
24. Dreuw A, Fleming GR, Head-Gordon M (2003) Phys Chem Chem Phys 5:3247
25. Starcke JH, Wormit M, Schirmer J, Dreuw A (2006) Chem Phys 329:39
26. Dreuw A, Weisman JL, Head-Gordon M (2003) J Chem Phys 119:2943
27. Dreuw A, Head-Gordon M (2004) J Am Chem Soc 126:4007
28. Pascal AA, Liu Z, Broess K, van Oort B, van Amerongen H, Wang C, Horton P, Robert B, Chang W, Ruban A (2005) Nature 436:134
29. Ruban AV, Berera R, Ilioaia C, van Stokkum IHM, Kennis JTM, Pascal AA, van Amerongen H, Robert B, Horton P, van Grondelle R (2007) Nature 450:575–578
30. Wormit M, Harbach PHP, Mewes JM, Amarie S, Wachtveitl J, Dreuw A (2009) BBA Bioenergetics 1787:738
31. Marian CM, Gilka N (2008) J Chem Theory Comp 4:1501–1515
32. Wormit M, Dreuw A (2006) J Phys Chem B 110:24200–24206
33. Wormit M, Dreuw A (2007) Phys Chem Chem Phys 9:2917
34. Dreuw A (2006) Chem Phys Chem 7:2259
35. Rogl H, Kühlbrandt W (1999) Biochemistry 38:16214–16222
36. Schubert A, Beenken WJD, Stiel H, Voigt B, Leupold D, Lokstein Heiko (2002) Biophys J 82:1030–1039
37. van Amerongen H, van Grondelle R (2001) J Phys Chem B 105:604–617